Holographic data storage in phenanthrenequinone doped PMMA

Gregory J. Steckman, Iouri Solomatine, Gan Zhou, Demetri Psaltis

Dept. of Electrical Engineering, California Institute of Technology, MS 136-93, Pasadena, CA 91125

ABSTRACT

Phenanthrenequinone (PQ)-doped poly(methyl methacrylate) (PMMA) is a photopolymer holographic recording material that can be made in large thicknesses and does not exhibit any shrinkage. Holograms are made permanent by a post-recording diffusion amplification process. PQ-doped PMMA thus exhibits many properties which make it an ideal candidate as a high-density read-only holographic data storage medium.

Recently we reported the holographic recording characteristics of phenanthrenequinone (PQ) doped PMMA.[1] We now demonstrate the holographic storage of binary data in this material. Shift multiplexing is used to store multiple holographic data pages in millimeter thick material samples. Each data page consists of a random array of binary 40 micron pixels. Recording is performed near the Fourier transform plane of the data mask, allowing high bit-densities to be achieved. The signal to noise ratio of stored data pages is used as an indication of hologram quality and data integrity. Bit density limitations are discussed with respect to the current performance of the recording material.

Keywords: holography, data storage, phenanthrenequinone, shift-multiplexing

1. INTRODUCTION

This paper first reviews the characterization of phenanthrenequinone (PQ) doped PMMA as a recording material for holographic memories. Holographic data storage utilizing shift-multiplexing is then demonstrated. Finally, data storage density limitations are investigated with respect to recording geometry, material thickness and dynamic range, and scatter noise.

The material consists of the polymer host matrix with added PQ molecules as photosensitive dopant. We have made high optical quality samples of this material with variable thicknesses, up to 5 mm, and in a variety of shapes. The material does not shrink after exposure, is inexpensive, durable, and lightweight, making it an attractive candidate for disk based holographic memory systems. Sample preparation consists of dissolving PQ molecules in liquid methyl methacrylate together with a polymerization initiator. This solution is then poured into molds and polymerized in an argon atmosphere at an elevated temperature. The molding process allows samples to be fabricated in a variety of geometries. Disks ranging between 2.5 cm to 10 cm in diameter with 1-5 mm thicknesses have been made. Figure 1 shows absorption spectra for doped and undoped PMMA before and after exposure for 1-mm-thick samples. The PQ-doped samples contained 0.7% of PQ molecules by weight.

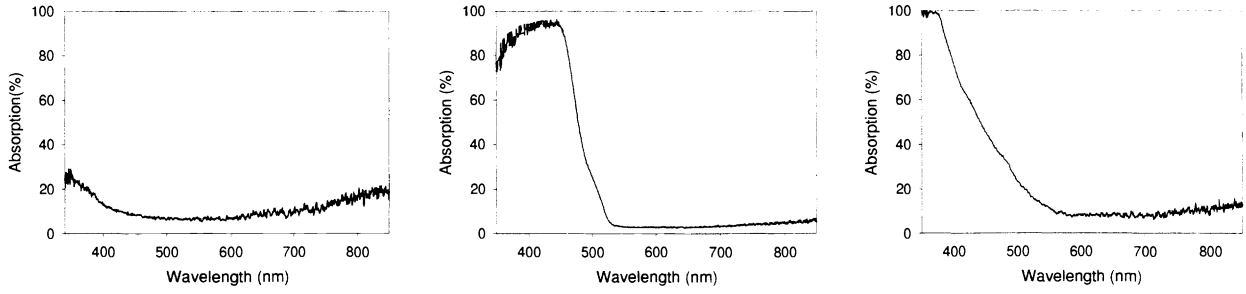

Figure 1: Absorption spectra for undoped PMMA (a), unexposed PQ-doped PMMA (b), and PQ-doped PMMA exposed to 488nm light (c).

Part of the SPIE Conference on Organic Photonic Materials and Devices
San Jose, California • January 1999
SPIE Vol. 3623 • 0277-786X/99/$10.00

2. HOLOGRAPHIC RECORDING

A hologram was recorded by a pair of 488 nm beams, each incident upon the material at an outside angle of 21.5°. The growth of the hologram was monitored during recording by probing the sample with a Bragg-matched He-Ne laser beam. Figure 2 shows the diffraction efficiency (diffracted power divided by the incident power) during recording in 1 mm thick material. The

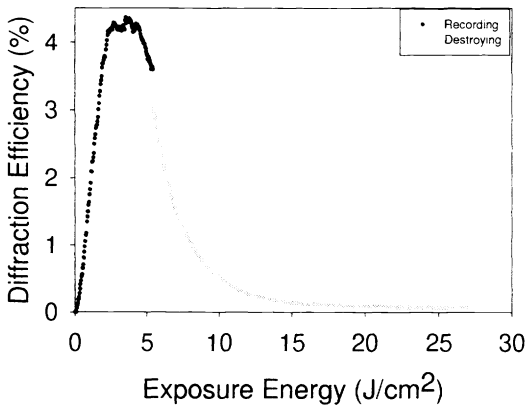

Figure 2: Diffraction efficiency versus exposure energy as the hologram is being recorded.

diffraction efficiency reached a maximum of 4.3% for an exposure energy of 2.5 J/cm^2. If exposure was allowed to continue, the diffraction efficiency began to drop. After 20 J/cm^2 of exposure with a single beam the hologram has decayed to approximately 0.1%. At this point the material was completely exposed and no more holograms could be recorded.

Permanent holograms that do not decay with subsequent illumination are recorded by stopping the exposure before saturation is reached and then baking the sample. Figure 3 shows the strength of a hologram as a function of baking time at a temperature

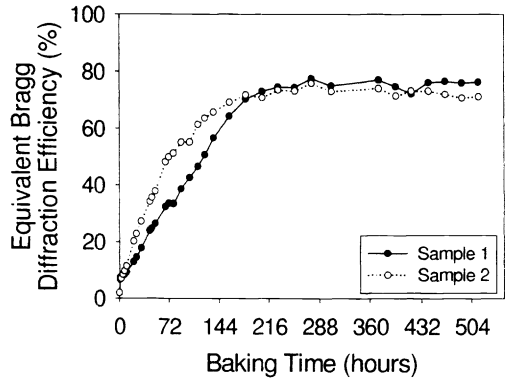

Figure 3: Diffraction efficiency versus baking time for a hologram exposed to 1 J/cm^2 of energy.

of 55° centigrade. The diffraction efficiency reaches a maximum after 12 days and remains steady with continued baking.

Figure 4 shows the selectivity curves for a weak and a strong hologram (2% and 35% diffraction efficiency, respectively). The 2% hologram has the sinc-squared selectivity curve as expected for a 1 mm thick hologram. The stronger hologram on the other hand has a selectivity curve which is distorted and shifted. For a holographic memory the diffraction efficiency is relatively small because many holograms are multiplexed. Therefore, this effect is not going to be observed in practice. For characterization purposes, the diffraction efficiency shown in figures 3 and 5 is calculated as the peak of the ideal Bragg selectivity curve with the same area as that of the measured curve. We attribute the slight shift of the weak hologram to a re-positioning

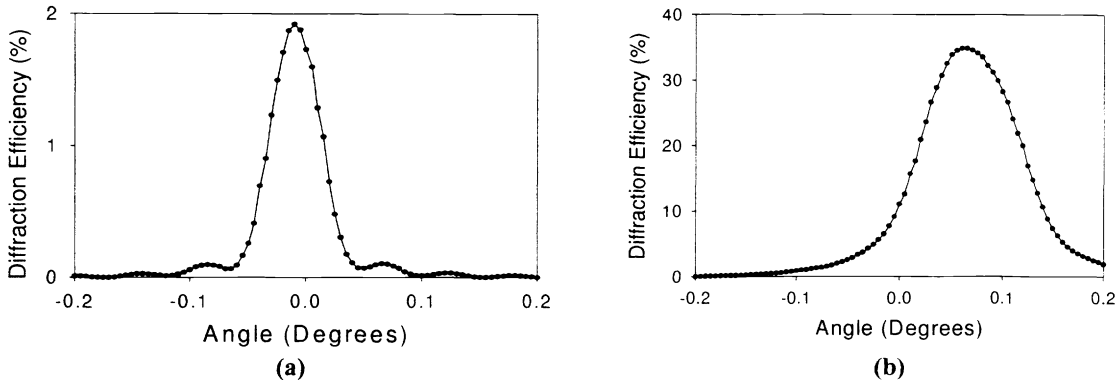

Figure 4: Selectivity curves for a 1 mm thick sample for a weak (a) and strong (b) hologram.

error arising from the removal of the material from the optical setup for baking. Shrinkage is not a suspect because of the ability to completely reconstruct high-bandwidth holograms.

The recording sensitivity has been measured for 1mm and 3mm thick samples as a function of exposure energy and is shown in Figure 5. For each exposure energy two holograms were recorded, each in a different sample of recording material, and then

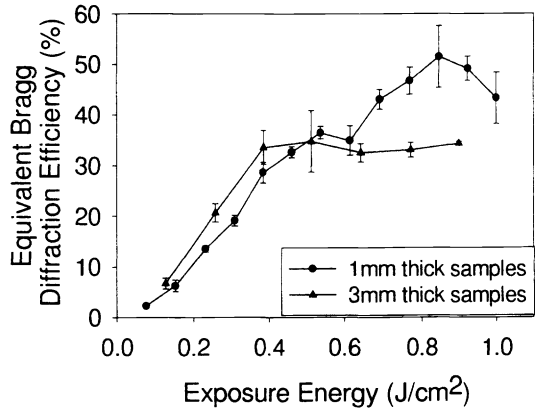

Figure 5: Exposure sensitivity of 1 and 3 mm thick samples.

baked for 48 hours at 55° centigrade to partially reveal the holograms. Plotted is the average of the equivalent diffraction efficiencies of the two trials with their standard deviation used as the error. For 1 mm thick samples the maximum diffraction efficiency was achieved with an exposure energy of 0.9 J/cm^2. For 3 mm thick samples the recording saturated after only 0.4 J/cm^2. In a separate experiment, several holograms were recorded with varying beam intensities while keeping the exposure energy constant. Over the range of 2 to 40 mW/cm^2 the material's recording sensitivity is not strongly dependent on the intensities of the recording beams.

Subsequent exposure causes erasure of previously recorded holograms as in photorefractives, however repeated exposure causes the material to saturate as in many other photopolymers. In order to design a strategy for recording multiple holograms in this material we must briefly discuss the physical mechanism involved. On illumination the PQ molecules are photoexcited and bond to the host PMMA matrix. When illuminated with two interfering beams, this bonding occurs primarily in regions of constructive interference. Through this process two partially offsetting gratings are created, one consisting of regions of photoexcited PQ molecules bonded to the host polymer and the other of PQ molecules that are not bonded to the host polymer. At room temperature there is minimal diffusion of the PQ molecules through the polymer matrix. During heating, the free PQ molecules diffuse and distribute evenly, revealing the hologram. The diffusion time depends both on the grating frequency and

the temperature.[2] A final uniform exposure causes all of the remaining free PQ molecules to bond to the PMMA matrix, thereby preventing any further holographic recording from taking place in the material.

We recorded with equal exposure energy 50 plane wave holograms at a single location of 3 mm thick samples, using peristrophic multiplexing.[3] We summed the square root of the measured diffraction efficiencies to form the cumulative grating strength,[4] defined as

$$C = \sum_{i=1}^{M} \sqrt{\eta_i}. \quad (1)$$

We then varied the cumulative exposure energy by increasing the exposure time of the individual holograms. Figure 6 shows

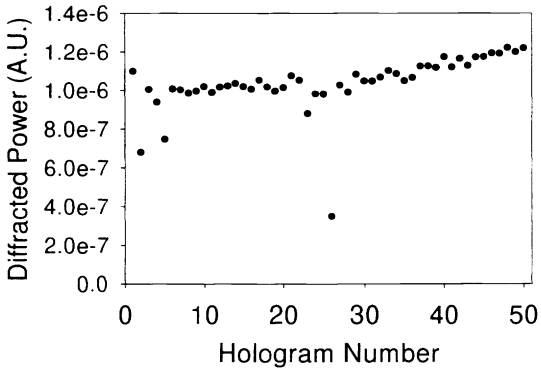

Figure 6: Strength of 50 holograms recorded in a 3 mm thick sample.

the strengths of the 50 holograms recorded in a single sample. The cumulative grating strength with the 50 holograms recorded to different total exposure energies for different samples is shown in Figure 7.The saturation value of the cumulative grating

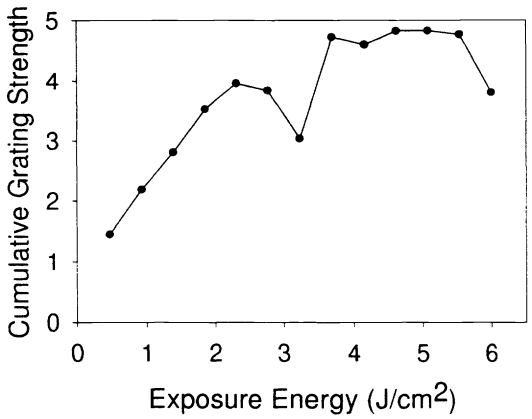

Figure 7: Cumulative grating strengths for 50 holograms in 3 mm thick samples with varying exposure energy

strength is approximately equal to the M/# of the material.[5] The M/# reaches a maximum of M/4.8 for a cumulative exposure energy of about 5 J/cm^2. With increased exposure energies the cumulative grating strength then begins to drop as a result of the hologram destruction process. The earlier recorded holograms are reduced in strength by the recording of subsequent holograms, and overpowers the increase gained by recording for longer exposure energies.

3. DATA STORAGE

Figure 8 is a schematic of the optical system used to demonstrate the storage of binary data pages in PQ-doped PMMA. A

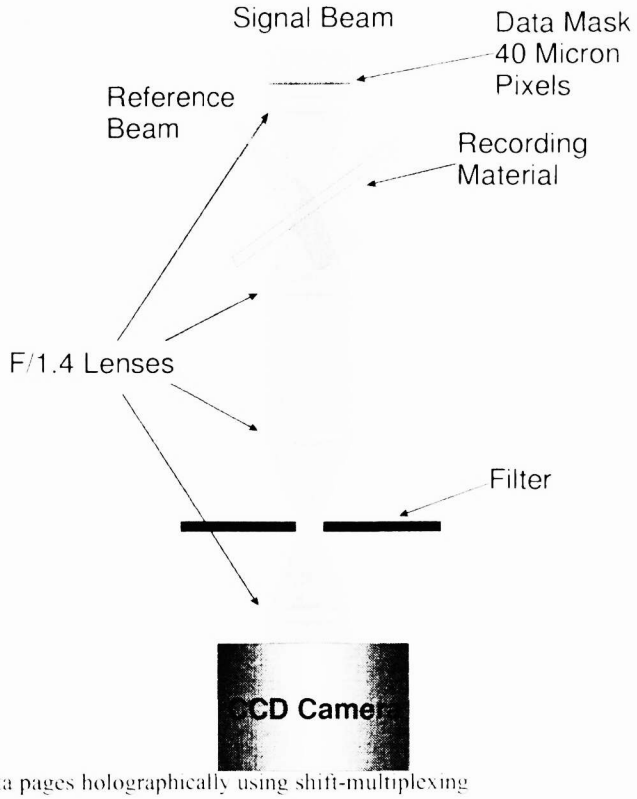

Figure 8: Optical setup for storing data pages holographically using shift-multiplexing

chrome-on-glass mask of a random 2-d array of 40 micron pixels is used as the data page to be stored. The recording material is placed on a motorized translation stage just behind the Fourier-plane of the first lens. The next two lenses form an imaging system of the Fourier transform to the plane of the filter. The filter is used to partially block scattered light from the recording material and acts to decrease the noise due to scattered light. A final lens is then used to image the reconstruction of the data mask onto a CCD detector. To implement shift multiplexing, a spherical reference beam, incident normal to the surface of the recording material, is used. Multiple partially overlapping holograms are recorded by translating the recording material between hologram exposures. The amount of shifting required to minimize cross-talk between recorded data pages is determined by the distance of the reference beam focal point from the material, z, and the angle between signal and reference beams, θ, and is given roughly as[6]

$$\delta = \frac{z\lambda}{L\tan\theta} \tag{2}$$

where L is the thickness of the recording material.

In order to judge the signal quality of the stored data pages the signal-to-noise ratio (SNR) is measured from reconstructed holograms. With this optical system there is not a one-to-one correspondence between data mask pixels and CCD pixels, with each data mask pixel occupying a square region approximately 4 pixels on a side. To calculate the SNR a portion of the reconstruction image is separated into a grid of 20 x 20 super-pixels, each occupying the area of multiple CCD pixels but a single data-mask pixel. The CCD pixels then falling on the boundary between two super-pixels are discarded, and the remaining CCD pixels are averaged to form the super-pixel values. The SNR is then calculated as

$$\mathrm{SNR} = \frac{\mu_1 - \mu_0}{\sqrt{\sigma_1^2 + \sigma_0^2}} \tag{3}$$

where μ are the means and σ are the standard deviations of the 1 and 0 valued super-pixels.

To get a baseline measurement for comparison purposes, the SNR of the optical system without the recording material in place was measured first, and a value of about 16 is obtained. Figure 9 is a plot of this value together with SNR measurements of

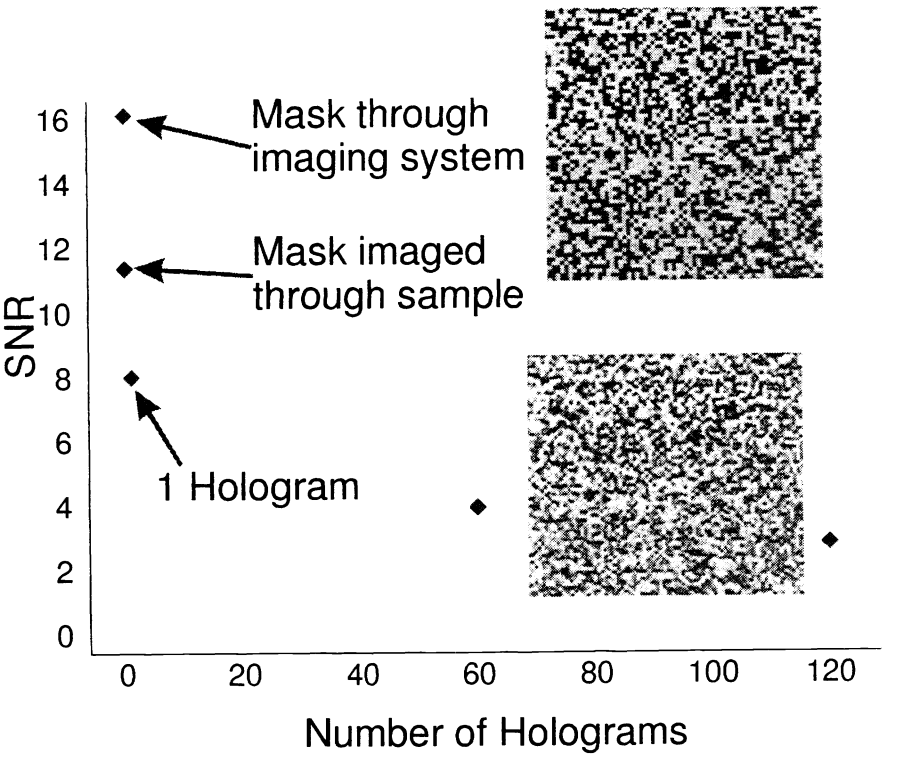

Figure 9: Signal-to-noise ratios for holographic data storage system using PQ doped PMMA as the recording material

several other conditions. The SNR of the optical system was also measured when only a sample of the recording material was in place, but a hologram had not been recorded. It is seen that insertion of the material decreases the SNR by approximately 25%, to about 12, however the value obtained is still high enough to avoid bit-errors. The reconstruction of a single, fairly strong, hologram yields an SNR of 8. Under these conditions there is no crosstalk noise, and the drop in SNR can be contributed to scatter noise, Bragg-mismatch due to removal of the sample from the optical system for baking, and grating distortion that may have occurred in the sample.

With an increase in the number of overlapping holograms the SNR decreases primarily for two reasons. First there is crosstalk between recorded holograms. Second the diffraction efficiency of each hologram decreases as $1/M^2$ where M is the number of overlapping holograms. It is this seconds source of SNR degradation which causes the most problems due to the scatter noise generated by the reference beam passing through the material to reconstruct the holograms. In the case of 120 holograms, the diffraction efficiency was approximately 7×10^{-4}, however the scattering level was approximately 3×10^{-4}. Ultimately there is a trade-off between SNR and the number of holograms which can be stored, and is the topic of the next section.

4. DENSITY LIMITATIONS

As was shown experimentally in section 3, as the number of holograms increases there is a corresponding decrease in the SNR. The limit to the number of allowable overlapping holograms ultimately limits the data storage bit-density for any given optical system. Since the strength of the recorded holograms depends on the recording material M/#, the number of holograms which may be overlapped depends on the M/#. The analysis below differs from those performed previously[7] by incorporating

not only selectivity considerations, but also dynamic range limitations through material M/# and each hologram's required diffraction efficiency.

In the calculation of data storage density, the holographic recording system is assumed to be composed of a set of identical lenses. The F-number of the lens is used to provide a relation between the lens, the number of pixels per data page, and the size of those pixels, such that the pixels can be adequately imaged by the optical system. Referring to Figure 10, the data mask

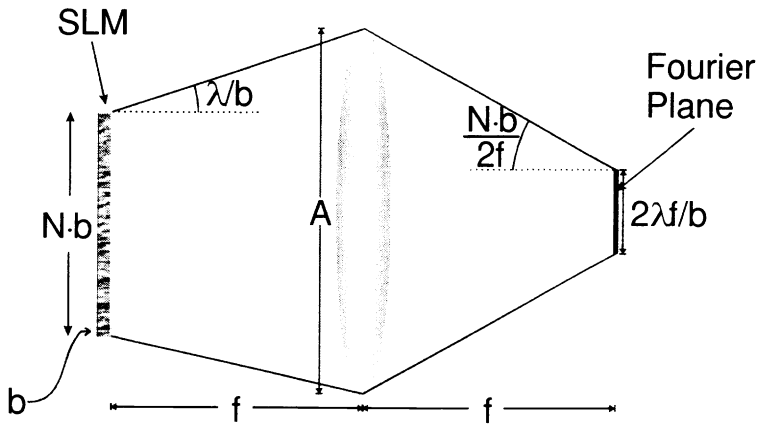

Figure 10: Model of pixels being imaged by a lens to the Fourier plane

(SLM) is placed one focal length in front of the lens of diameter A and focal length f. The SLM contains N pixels on a side, each square with side of length b. The wavelength of illumination is λ. Assuming the paraxial approximation, the pixels cause the illumination incident on the SLM to diffract with an angle of λ/b. In order for all of the light diffracted from the outer-most pixel to pass through the lens, the relation

$$N = \frac{A}{b}\left(1 - 2\frac{\lambda}{b}\mathrm{f/\#}\right) \tag{4}$$

must be satisfied. At the back focal plane of the lens appears the Fourier transform of the SLM which has a width of approximately $2\lambda f/b$ diverging with an angle of $Nb/(2f)$.

With this geometry the width of the signal beam on the front surface of the recording material, incident at an angle θ_s, is given by

$$W_f = \frac{2\lambda f}{b}\left[\cos(\theta_s) + \sin(\theta_s)\tan\left(\theta_s + \frac{Nb}{2f}\right)\right]. \tag{5}$$

Taking into account the index of refraction for the recording material with thickness L, the width of the signal at the back surface of the material is given by:

$$W_b = W_f + L\left\{\tan\left[\mathrm{asin}\left(\sin\left(\theta_s + \frac{Nb}{2f}\right)/n\right)\right] - \tan\left[\mathrm{asin}\left(\sin\left(\theta_s - \frac{Nb}{2f}\right)/n\right)\right]\right\} \tag{6}$$

The reference beam is selected with numerical aperture (NA) and focal position so as to completely cover the signal beam on the front and back surfaces of the material. The selection of the best NA and the choice of focal position must be taken into account with the shift selectivity given by Equation 2 and the limit placed on the number of allowable overlapping holograms, given by

$$M = \mathrm{M/\#}/\sqrt{\eta} \tag{7}$$

where η is the minimum allowable diffraction efficiency per hologram. An optimal reference beam exists such that the selectivity obtained yields the same number of overlapping holograms as given by Equation 7. If the selectivity is better than that required by Equation 7 then the focal position is closer to the material than it needs to be and the NA is therefore higher in order to cover the signal, which results in more area consumed by the reference beam, causing a decrease in storage density.

The final data storage density is

$$D = \frac{N^2}{\delta \cdot W_b} \tag{8}$$

where δ is the distance shifted in the plane of the reference and signal beams and W_b is the distance shifted in the out-of-plane direction.

The storage density was calculated using the values from the experimental system of section 3 and numerically optimizing the density by varying the reference beam NA and focal point location. Figure 11 shows a plot of the density as a function of mate-

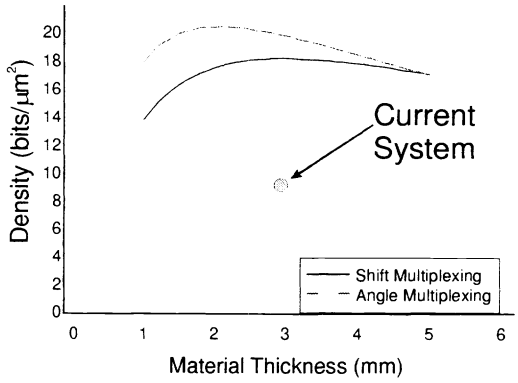

Figure 11: Optimal storage density possible with the system from section 3

rial thickness, where the M/# was assumed to vary linearly with thickness, having a value of 2.5 at 3 mm. For comparison the density was also computed for angle multiplexing with a signal beam normal to the material and reference beam off-axis. The exact system used in section 3 is labeled at 9 bits per square micron. The projected optimal for this shift-multiplexed setup is about twice this, at 18 bits per square micron. The difference arises because the minimum required diffraction efficiency for the calculated densities was set at 10^{-4}, while the actual system required a diffraction efficiency of 7×10^{-4} in order to obtain an acceptable SNR. Furthermore, the reference beam used was not optimal.

To see the effects of a decrease in the required diffraction efficiency (or the equivalent case of an increase in M/#), the density was computed as a function of required diffraction efficiency for 3 mm thick material with an M/# of 2.5, and is plotted in Figure 12. As expected, with a decrease in the required diffraction efficiency the storage density increases. For both shift and

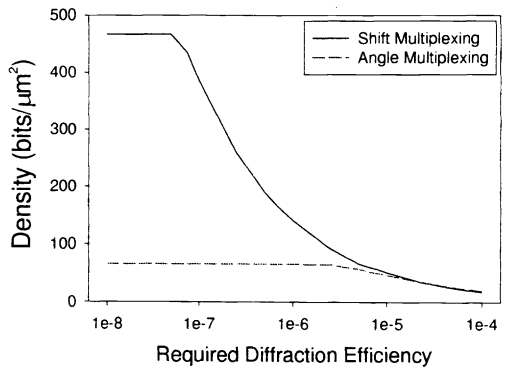

Figure 12: Optimal storage density as a function of required diffraction efficiency

angle multiplexing the saturated level occurs when the geometry limits the number of holograms due to selectivity. Here, angle multiplexing is lower than it could be since the reference beam was assumed to be constrained to one side of the signal beam, and only transmission holograms are recorded, which is often the case for actual systems.

5. CONCLUSION

The basic holographic recording characteristics, for single and multiple overlapped holograms, for phenanthrenequinone-doped PMMA have been described. High-optical-quality, thick (5 mm) samples were made and have been shown to exhibit long-term permanent holographic storage through temperature cycling. A value of M/4.8 was experimentally measured for 3 mm thick samples. Binary data pages were stored holographically in the material with a bit density of 9 bits/μm^2 and an SNR of approximately 2.5. The theoretical data storage capacity of shift and angle-multiplexing systems was calculated with the inclusion of M/# and a minimum required diffraction efficiency per hologram. For an M/# limited material such as PQ-doped PMMA, scatter noise is the primary factor limiting data storage density.

ACKNOWLEDGMENTS

This work was supported by TRW as part of the Neuromorphic Systems Engineering Research Center, Rome Labs, and by the U.S. Air Force Office of Scientific Research.

REFERENCES

1. G. J. Steckman, I. Solomatine, G. Zhou, and D. Psaltis, "Characterization of phenanthrenequinone-doped poly(methyl methacrylate) for holographic memory," Opt. Lett. **23**:(16), pp.1310-1312, 1998.

2. A. V. Veniaminov, V. F. Goncharov, and A. P. Popov, "Hologram amplification by diffusion destruction of out-of-phase periodic structures," Opt. Spektrosk. **70**, pp. 864-869, 1991.

3. K. Curtis, A. Pu, and D. Psaltis, "Method for holographic storage using peristrophic multiplexing," Opt. Lett. **19**:(13), pp. 993-994, 1994.

4. A. Pu, K. Curtis, and D. Psaltis, "Exposure schedule for multiplexing holograms in photopolymer films," Opt. Eng. **35**:(10), pp. 2824-2829, 1996.

5. D. Psaltis, D. Brady, and K. Wagner, "Adaptive optical networks using photorefractive crystals," Appl. Opt. **27**:(9), pp. 1752-1759, 1988.

6. G. Barbastathis, M. Levene, and D. Psaltis, "Shift multiplexing with spherical reference waves," Appl. Opt. **35**:(14), pp. 2403-2417, 1996.

7. H. Li and D. Psaltis, "3-Dimensional holographic disks," Appl. Opt. **33**:(17), pp. 3764-3774, 1994.